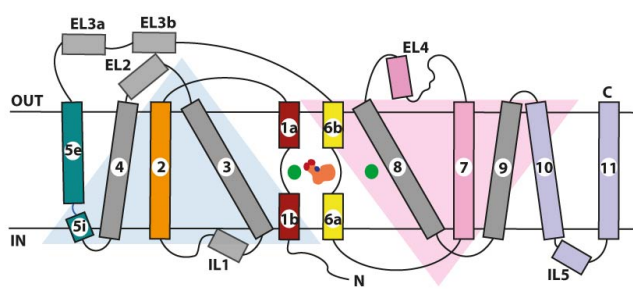
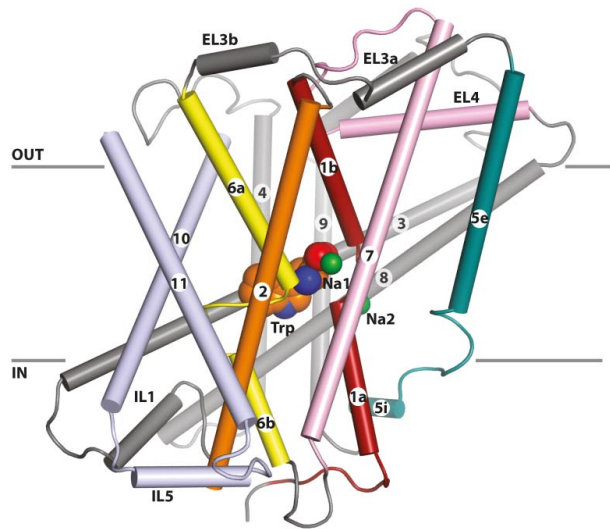
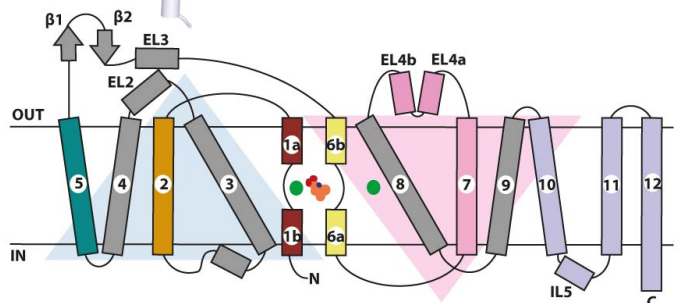
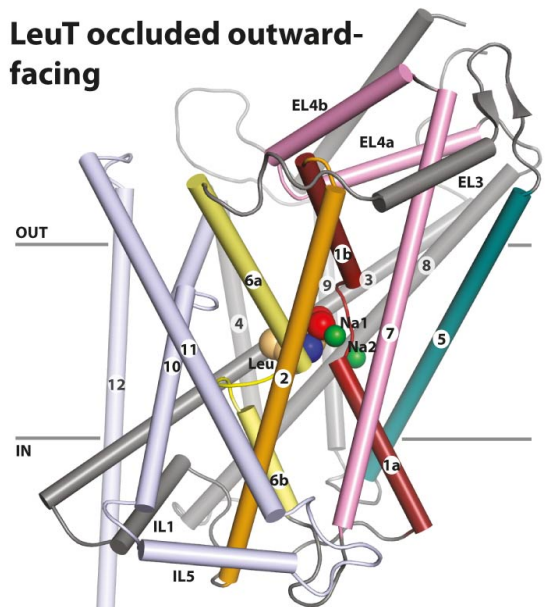


a MhsT occluded inward-facing



b LeuT occluded outward-facing

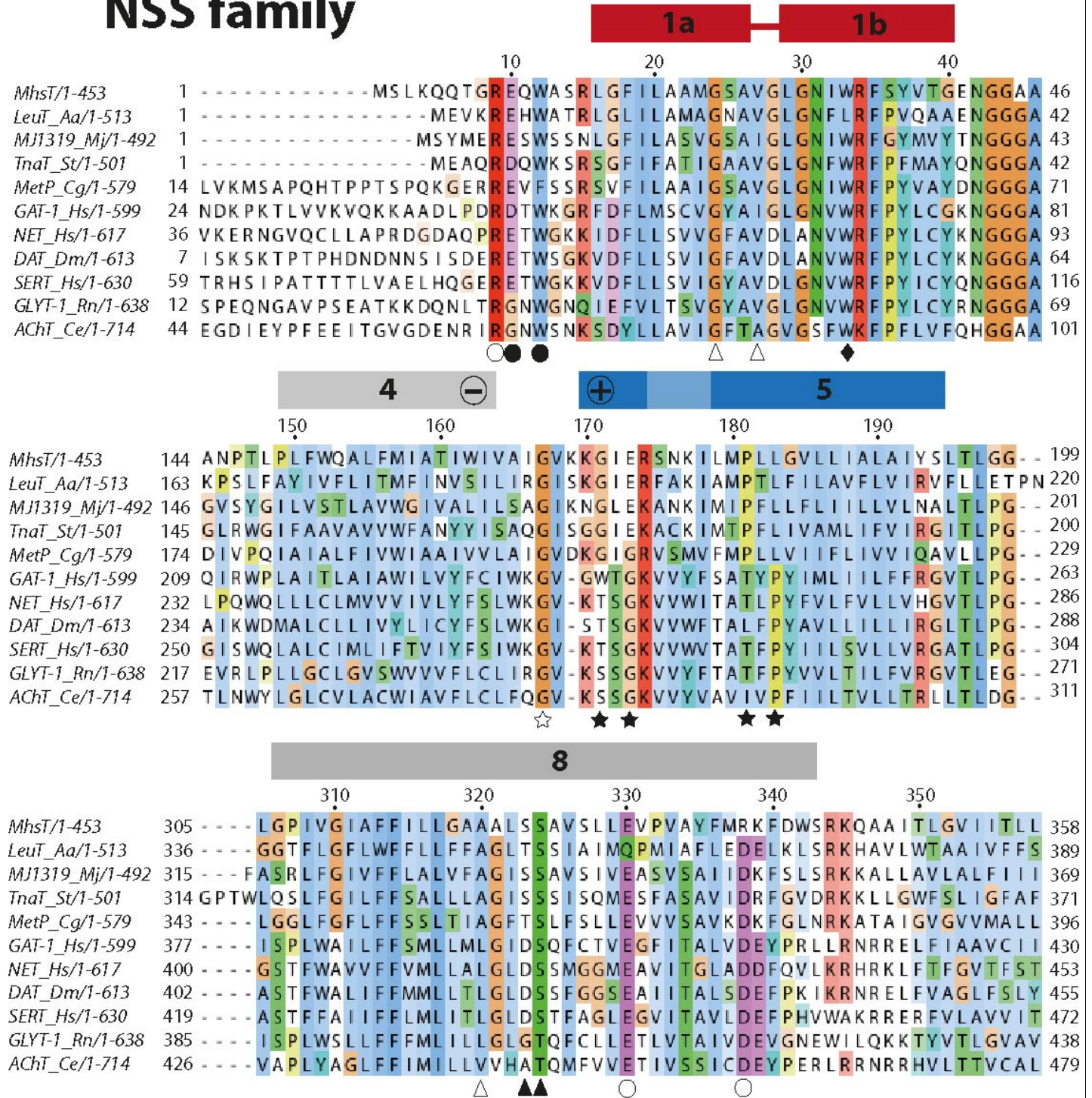


Supplementary Figure 1

MhsT and LeuT architecture.

a, Cartoon structure representation and topology diagram for MhsT in the occluded inward-facing state and **b**, LeuT in the occluded outward-facing state (PDB 2A65)⁷. Important structural elements for conformational changes between these states are highlighted. Color scheme: scaffold domain (TM 3-4, 8-9) – grey; bundle elements – TM1 red, TM6 yellow, TM7 and EL4 pink and TM2 orange; TM5 – cyan.

NSS family

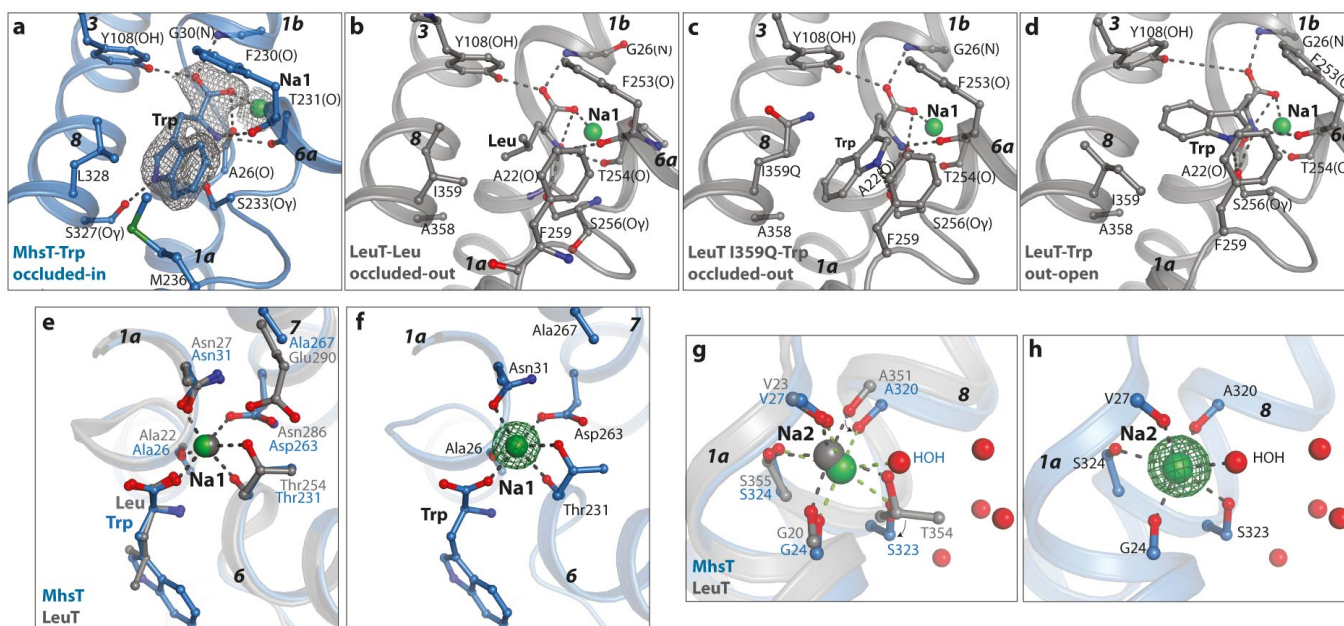


Supplementary Figure 2

Alignment of bacterial and eukaryotic members of the NSS family.

The sequence alignment of helices 1, 4, 5 and 8, which are involved in the formation of the Na₂ site and the cytoplasmic pathway leading to it, are shown. Bacterial NSS members: *MhsT*_Bh (multi-hydrophobic amino acid transporter, *Bacillus halodurans*, NP_241994), *LeuT*_Aa (leucine transporter, *Aquifex aeolicus*, O67854), *TnaT*_St (tryptophan transporter, *Symbiobacterium thermophilum*, O50649), *MetP*_Cg (methionine/alanine transporter, *Corynebacterium glutamicum*, Q8NRL8), *MJ1319*_Mj (hypothetical

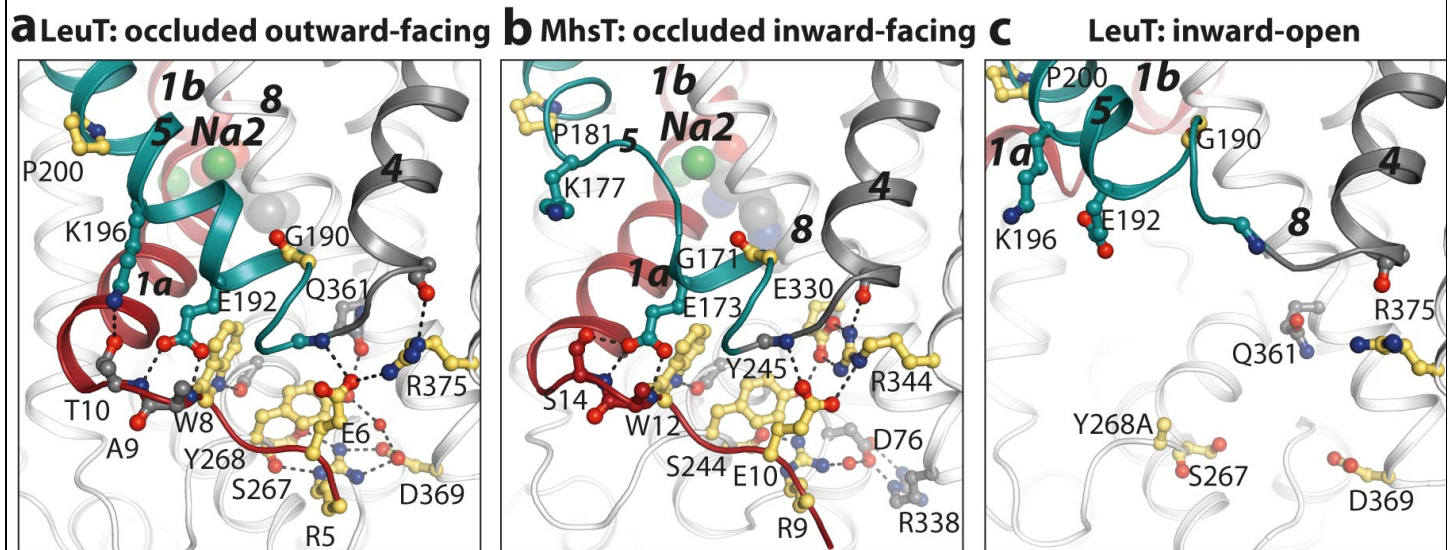
Na⁺-dependent transporter, *Methanococcus jannaschii*, Q58715); animal transporters: SERT_Hs (Na⁺-dependent serotonin transporter, *Homo sapiens*, P31645), NET_Hs (Na⁺-dependent noradrenaline transporter, *Homo sapiens*, P23975), DAT_Dm (Na⁺-dependent dopamine transporter, *Drosophila melanogaster*, Q9NB97), GLYT-1_Rn (Na⁺- and chloride-dependent glycine transporter 1, *Rattus norvegicus*, P28572) AChT_Ce (Na⁺-dependent acetylcholine transporter, *Caenorhabditis elegans*, O76689), GAT-1_Hs (Na⁺- and chloride-dependent γ -aminobutyric transporter 1, *Homo sapiens*, P30531). Helix positions are shown according to the MhsT structure with the unwound region of TM5 in light blue. The Na⁺ coordinating residues of Na2 are marked by triangles: residues that coordinate Na⁺ by side chains (filled) and by backbone atoms (empty). The intracellular gate residues are indicated by circles: salt bridges and a hydrophobic plug (filled) and residues interacting with dipoles of TM5 (+) and TM4 (-) (empty). The kink between TM4-5 (empty stars) and the TM5 helix breaking motif Gly(X₃₋₄)Gly(X₉)Pro (filled stars) are conserved among all NSS family members. The highly conserved Trp33^{MhsT} situated at the extracellular vestibule is indicated by diamond.



Supplementary Figure 3

Comparison of MhsT and LeuT substrate and Na⁺-binding sites.

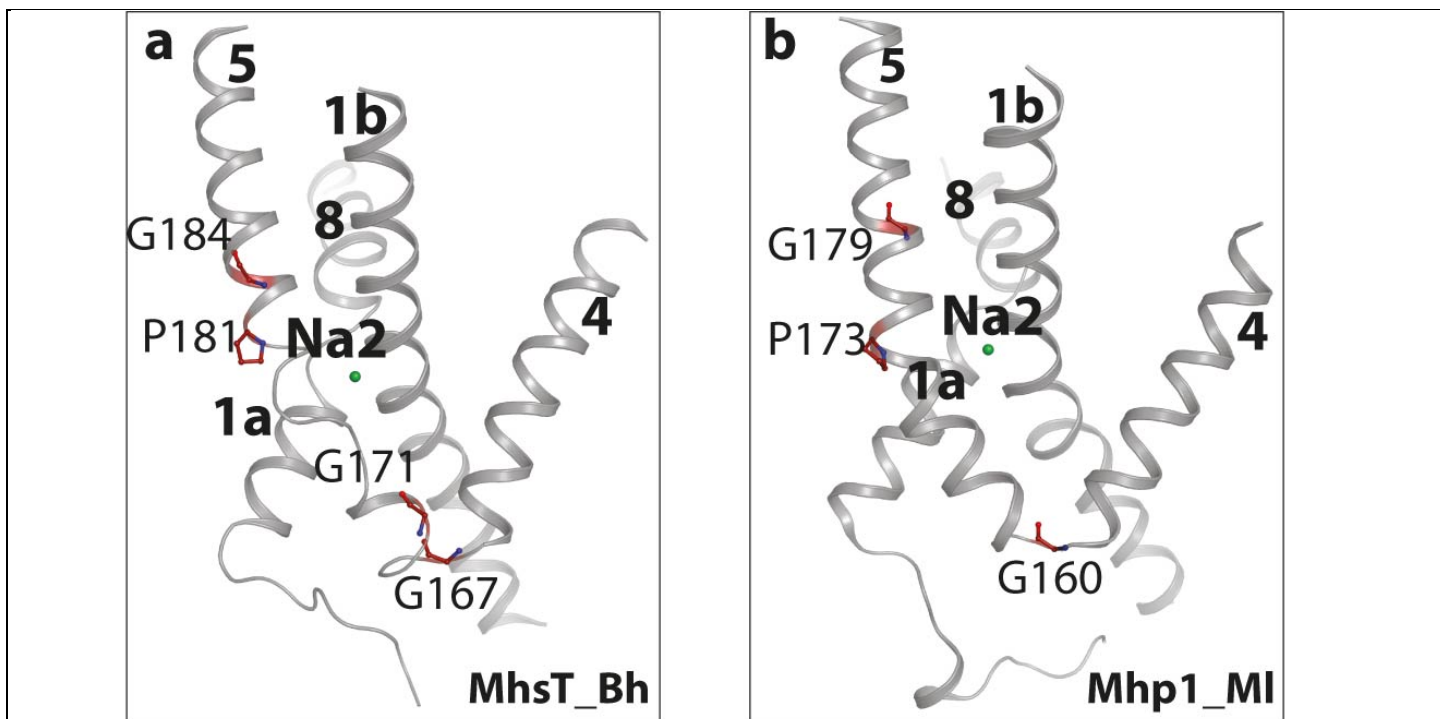
a, L-tryptophan (2F_o-F_c map at 2 r.m.s.d.) carboxyl and amino groups are bound at the MhsT active site through hydrogen bonds to the side chains of Tyr108, Ser233 and backbone atoms of Ala26, Gly30, Phe230 and Thr231. In addition the L-tryptophan carboxyl group coordinates Na⁺ at the Na1 site. The indole ring is bound only through a hydrogen bond to Ser327Oy. Met236 is moved away from the binding site, making space for the bulky L-tryptophan side chain. **b**, LeuT binding site with bound L-leucine in the occluded outward-facing state (PDB 2A65)⁷. **c**, LeuT mutation I359Q²⁹ allows L-tryptophan to bind in an occluded outward-facing state (PDB 3QS5)²⁹, but with a different rotamer than in the MhsT-Trp structure as seen in (a). **d**, Wild-type LeuT with bound L-tryptophan in an outward-open state (PDB 3F3A)⁸, where L-tryptophan pushes the LeuT binding site open. **e-h**, Na1 and Na2 binding sites in MhsT and LeuT. LeuT (PDB 2A65⁷, grey) and MhsT (this study, light blue) superimposed by structural alignment of scaffold helices (TM3-4, TM8-9) (**e** and **g**), and simulated annealing omit maps contoured at 5.0 r.m.s.d. for Na⁺ sites in MhsT (**f** and **h**). **e-f**, Structures of the Na1 site of MhsT and LeuT are similar, but MhsT has an additional negative charge – Asp263 (Asn286^{LeuT}). LeuT has a Glu290^{LeuT} residue one helix turn away from the Na1 site that was associated with proton antiport in bacterial NSS members⁶¹. At the equivalent position MhsT has Ala267, with no such capacity, thus Asp263 is a likely other candidate for this role in proton antiport⁶¹. **g-h**, The Na2 site of MhsT in the occluded inward-facing state exhibits a more open structure than the Na2 site in the LeuT occluded outward-facing state: helix 8 residues Ala320 and Ser323 are moved away from helix 1 making space for an additional ligand - a water molecule, which is in contact with the intracellular environment. The Na⁺ coordination geometry changes from trigonal-bipyramidal (LeuT, grey dashed lines) to octahedral (MhsT, light green dashed lines).



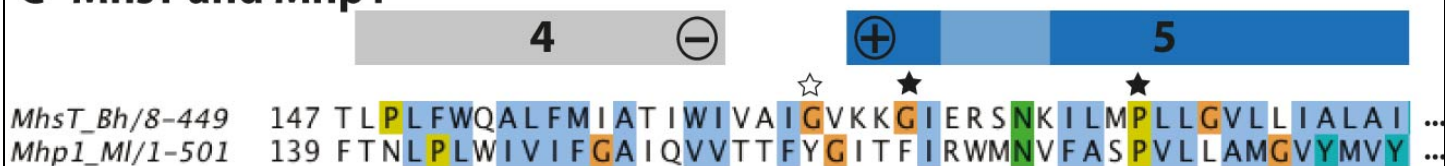
Supplementary Figure 4

The intracellular-gate interactions in MhsT and LeuT.

Dense network of conserved residues (yellow sticks) of TM1a (red), TM5 (cyan) and neighboring helices forming the intracellular gate. **a**, LeuT occluded outward-facing (PDB 2A65)⁷, **b**, MhsT occluded inward-facing, and **c**, LeuT inward-open (PDB 3TT3)¹⁰ states.



C MhsT and Mhp1



d NCS1 family

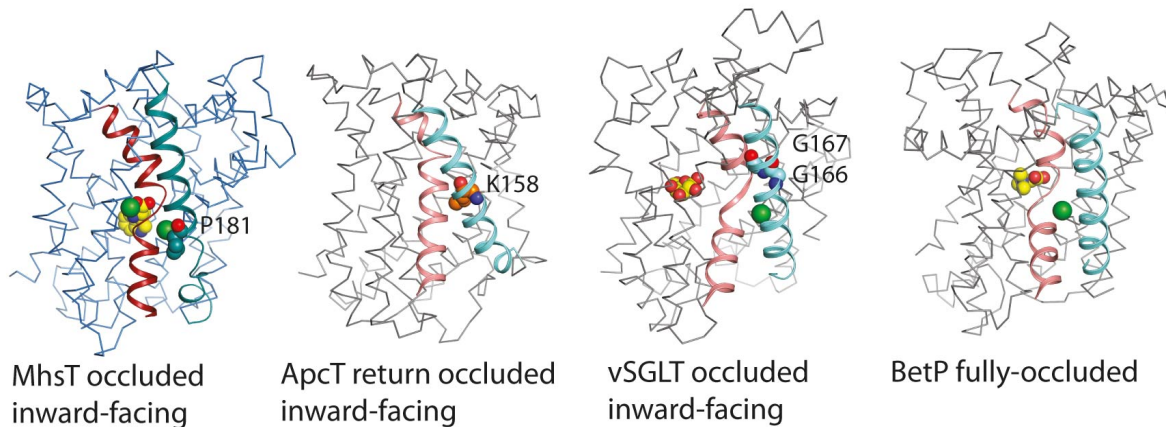


Supplementary Figure 5

A conserved TM5 proline in LeuT-fold transporters.

a-b, Comparison of TMs 1, 4, 5 and 8 of MhsT (occluded inward-facing) and Mhp1 occluded outward-facing (PDB 2JLO)¹⁵ structures. **c**, Structural alignment of MhsT occluded inward-facing and Mhp1_MI (benzyl-hydantoin transporter from *Microbacterium liquefaciens*, 210060745) occluded outward-facing (prepared by Chimera⁵⁹, helix position shown for MhsT) states. TM5 helix breaking Gly/Pro of MhsT are marked by stars: conserved GlyX₉Pro motif of the NSS family (filled) and the kink between TM4-5 (empty). **d**, Sequence alignment (generated with Muscle⁵⁷) of the nucleobase:cation symporter-1 (NCS1) family: HyuP_Aa (probable hydantoin permease of *Arthrobacter aurescens*, Q9F467); CodB_Ec (cytosine permease of *Escherichia coli*, P0AA82); Pucl_Bs (allantoin permease of *Bacillus subtilis*, NP_391528.1); MtlP_Sf (putative mannitol transporter of *Shewanella frigidimarina*, Q082R8); FycB_An (cytosine-purine-scavenging protein of *Aspergillus nidulans*, B1PXD0); Fcy21_Ca (hypoxanthine/adenine/guanine (purine) transporter of *Candida albicans*, Q708J7); YbbW_Ec (allantoin permease of *E. coli*, P75712). Conserved Pro of the NCS1 family marked as filled squares.

flexible Gly position as empty squares with helix positions shown for Mhp1. The sequence alignment was illustrated with Jalview⁵⁹. Note the correspondence of Gly/Pro residues in TM4-TM5 of Mhp1/NCS1 family to the Gly(X₃₋₄)Gly(X₉)Pro motif of NSS that suggests a similar TM5 unwinding mechanism for Na₂ release in the NCS1 family.



MhsT to ApcT

ApcT/3-435 148 ---G---RAEFF-IVLVKLLILGLFIFA-GLTI---HPSYV 178
MhsT/8-449 168 VKKGIER-SNKILMPLLVLLIALA-IYS-LT-LGGAKEGL 204

5

MhsT to vSGLT

vSGLT/3-514 152 -----V-VWT-DVIVQVFFLVGGFMTTYMAVSFI 178
MhsT/8-449 167 GVKKGIERSN-KILMPLLVLLIALAIYSLTLG 198

5

MhsT to BetP

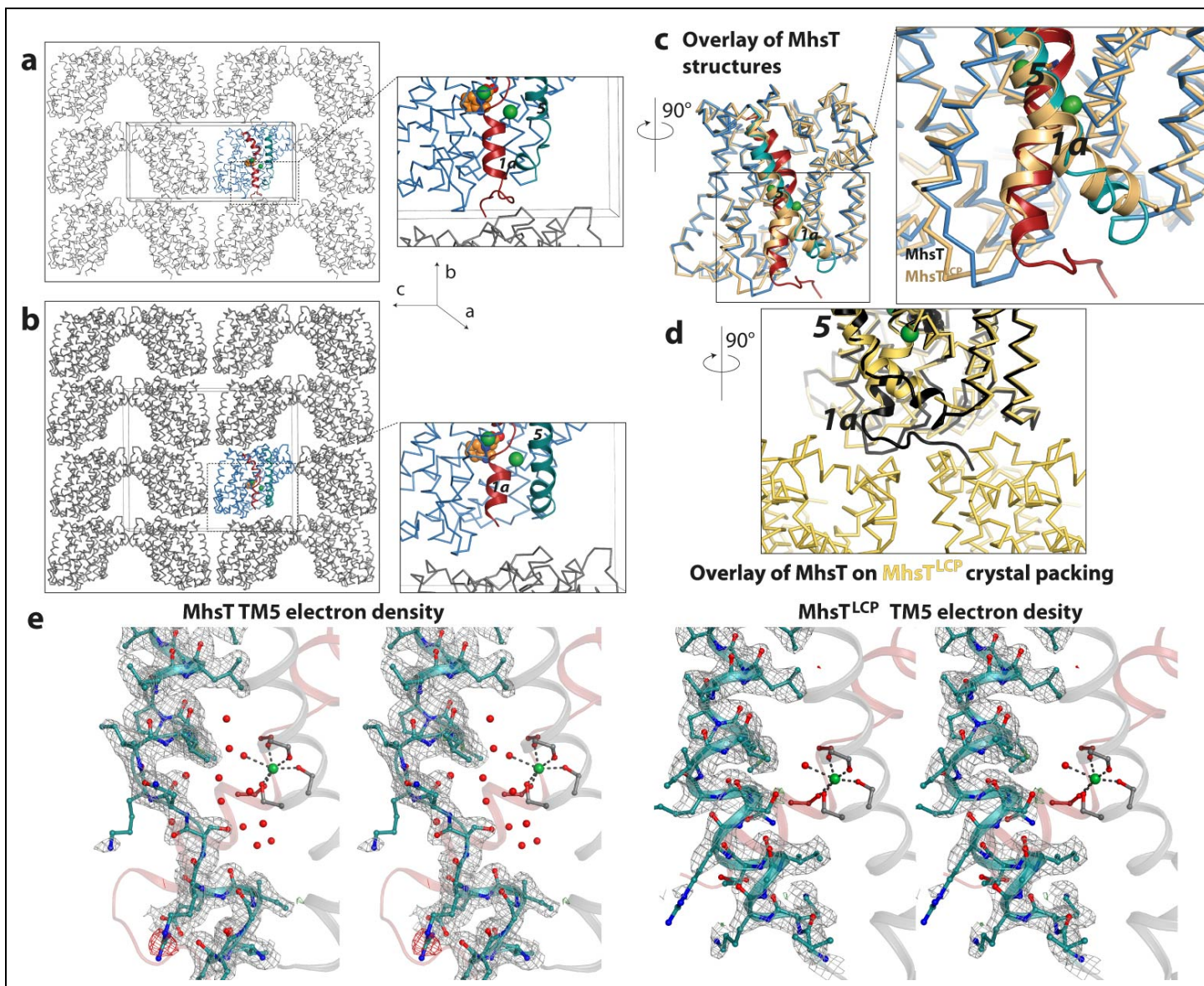
BetP/56-552 291 SGVVKGIQYL-SN-ANMVLAAALLAIFV-FVVG-P----- 320
MhsT/8-449 166 IGVKKGIERSN-KIL-MPLLVLLIALAI--YSLTLGGAKE 202

5

Supplementary Figure 6

Structural alignment of MhsT to ApcT, vSGLT and BetP prepared with DaliLite.

The structural alignment of MhsT to the LeuT-fold symporters: ApcT occluded inward-facing state (PDB 3GIA)¹⁶, vSGLT occluded inward-facing state (PDB 3DH4)¹⁴ and BetP fully-occluded state (PDB 4AIN chain B)¹⁷. TM1 is shown in red and pink, TM5 in cyan; substrates are shown as yellow spheres, Na⁺ ions as green spheres and proton binding residue for ApcT as orange spheres. The helix breaker in MhsT (Pro181) and potential helix breaker in vSGLT (Gly166-Gly167) are shown as cyan sphere. ApcT does not have any helix breaking residues in TM5, however the proposed H⁺ binding residue Lys158 is at a similar position (orange rectangle) to the Pro181 in MhsT (cyan rectangle). vSGLT in the crystal structure of occluded inward-facing state has missing residues at the TM4-TM5 turn (Tyr179-Gly180-Gly181-Leu182-Ser183-Ala184), probably due to their flexibility. Furthermore, vSGLT has two glycines (Gly166-Gly167, cyan rectangle) one helix-turn downstream from the Pro181 in MhsT. However, it is not clear if it would have similar effect as in MhsT. BetP does not have any glycines or prolines in TM5.



Supplementary Figure 7

Crystal packing of HiLiDe and LCP structures of MhsT.

a, Crystal packing of MhsT in the P2 crystal form from HiLiDe crystallization. The N-terminus of TM1a is unperturbed by the crystal packing and interacts with TM5. b, The C2 crystal form from lipid cubic phase crystallization. Crystal packing is tighter with the N-terminus displaced and disordered; TM5 adopts a less extended form as a near-continuous helix. c, Superposition of the two MhsT structures: the HiLiDe structure (grey, TM1a red, TM5 cyan) superimposed on the MhsTLCP (yellow). d, Superposition of MhsT HiLiDe structure (black) on LCP structure crystal packing (yellow) showing that the N-terminus is replaced by a loop of a neighboring molecule. e, Stereo view of TM5 electron density maps in MhsT HiLiDe and LCP structures.

Supplementary Note

The MhsT structural fold is similar to LeuT^{7,10} and dDAT¹¹. For the structural alignment of MhsT to the available LeuT structures^{7,10} DaliLite scores were 40-45 with r.m.s.d. values of 2.2-2.9 Å, whereas for LeuT occluded outward-facing to the inward-open state (as a control) the score was 48 and r.m.s.d. value of 2.4 Å (Supplementary Table 1). The structural alignment of dDAT¹¹ to LeuT outward-oriented states^{7,10} gave DaliLite scores of 38-40 and r.m.s.d. of 2.3-3.1 Å; whereas to the occluded inward-facing state of MhsT the DaliLite score was 36 with an r.m.s.d. of 3.1 Å; and to the LeuT inward-open state¹⁰ the DaliLite score was 29 and r.m.s.d. 3.8 Å. A structural alignment of MhsT to non-NSS LeuT-fold transporters⁶² gave DaliLite scores of 13-25 and r.m.s.d. values of 3.5-4.8 Å. Thus, bacterial members of the NSS family are closely related to eukaryotic NSS, and only remotely related to other LeuT fold transport families. This and the distribution of many critical and conserved residues at functional sites supports that the NSS transport mechanism is conserved across the family.

Mhp1 from the NCS1 family also displays a conserved TM5 GlyX_nPro pattern. Additionally, other LeuT-fold symporter structures also show a kinked TM5, e.g. for ApcT, where the proposed H⁺-binding residue Lys158^{ApcT} is situated in TM5¹⁶ at a similar position to Pro181^{MhsT} (Supplementary Fig. 6). However, compared to the release of Na⁺, which requires substantial rearrangements of protein elements, H⁺ release does not require large openings in the protein. Available structures of vSGLT in the occluded inward-facing and inward-open states do not reveal kinks, breaks or other structural changes in TM5 (Supplementary Fig. 6), although vSGLT has two conserved glycine residues, which are positioned one helix turn away from the position corresponding to Pro181^{MhsT} and could be important for flexibility in this region during transport (Supplementary Fig. 6). In BetP the entire TM5 helix moves to close the extracellular side and open the cytoplasmic passage for substrate release¹⁷, and there are no helix breaking residues at TM5 (Supplementary Fig. 6).

Supplementary Tables

Supplementary Table 1. Superposition of MhsT occluded inward-facing state with LeuT and *Drosophila* dopamine transporter (dDAT). The structures were superimposed using the overall structure (TM1-11)* with the PYMOL ‘super’ algorithm and DaliLite⁵⁷.

| Superposed structures | Overall Ca, r.m.s.d., Å (aligned residues) | DaliLite r.m.s.d., Å overall Ca (aligned residues) | DaliLite Z-score [#] |
|---|--|---|-------------------------------|
| Superposition to MhsT occluded inward-facing | | | |
| LeuT outward-open (PDB 3TT1) ¹⁰ | 3.3 (410) | 2.9 (422) | 40.2 |
| LeuT occluded outward-facing (PDB 2A65) ⁷ | 2.3 (382) | 2.3 (423) | 44.9 |
| LeuT inward-open (PDB 3TT3) ¹⁰ | 1.8 (332) | 2.2 (404) | 39.1 |
| dDAT outward-open (PDB 4M48) ¹¹ | 4.2 (379) | 3.1 (406) | 35.6 |
| Superposition to LeuT occluded outward-facing (PDB 2A65) ⁷ | | | |
| LeuT inward-open (PDB 3TT3) ¹⁰ | 1.9 (444) | 2.4 (487) | 48.7 |
| dDAT outward-open (PDB 4M48) ¹¹ | 2.3 (381) | 3.1 (447) | 37.5 |
| Superposition to dDAT outward-open (PDB 4M48) ¹¹ | | | |
| LeuT outward-open (PDB 3TT1) ¹⁰ | 1.4 (343) | 2.3 (466) | 40.4 |
| LeuT inward-open (PDB 3TT3) ¹⁰ | 4.1 (421) | 3.8 (452) | 28.5 |

* MhsT residues: 8-448; LeuT residues: 5-477

[#] Dali Z-score measures the significance of the detected structural similarity based on an experimentally determined background distribution of dali scores and is normalized according to the size of the domain^{63,64}.

Supplementary Table 2. Comparison of the distance from Na⁺ to coordinating residues in LeuT and MhsT. Three LeuT structures: outward-open (PDB 3F3A)⁸ with two bound Na⁺ and L-Trp, outward-open with two Na⁺ (PDB 3TT1)¹⁰ and occluded outward-facing with two Na⁺ and L-Leu (PDB 2A65)⁷; compared to the occluded inward-facing MhsT structure.

| Distance from Na ⁺ to coordinating residues (Å) | LeuT:2Na:Trp in outward-open state (PDB 3F3A) | LeuT:2Na in outward-open state (PDB 3TT1) | LeuT:2Na:Leu in occluded outward-facing state (PDB 2A65) | MhsT:2Na:Trp in HiLiDe occluded inward-facing state | MhsT:2Na:Trp in LCP occluded inward-facing state |
|--|---|---|--|---|--|
| Na1 to | | | | | |
| A22(O) ^{LeuT} /A28(O) ^{MhsT} | 2.4 | 2.4 | 2.2 | 2.2 | 2.2 |
| N27(Oδ) ^{LeuT} /N33(Oδ) ^{MhsT} | 2.6 | 2.5 | 2.2 | 2.6 | 2.4 |
| T254(O) ^{LeuT} /T233(O) ^{MhsT} | 2.5 | 2.4 | 2.3 | 2.5 | 2.4 |
| T254(OY) ^{LeuT} /T233(OY) ^{MhsT} | 2.7 | 2.4 | 2.4 | 2.5 | 2.4 |
| N286(Oδ) ^{LeuT} /263(Oδ) ^{MhsT} | 2.4 | 2.4 | 2.5 | 2.5 | 2.5 |
| Leu(O) ^{LeuT} /Trp(O) ^{MhsT} | 2.7 | – | 2.5 | 2.5 | 2.5 |
| Na2 to | | | | | |
| G20(O) ^{LeuT} /G24(O) ^{MhsT} | 2.3 | 2.5 | 2.2 | 2.1 | 2.3 |
| V23(O) ^{LeuT} /V27(O) ^{MhsT} | 2.3 | 2.1 | 2.2 | 2.4 | 2.4 |
| A351(O) ^{LeuT} /A320(O) ^{MhsT} | 2.3 | 2.0 | 2.3 | 2.4 | 2.1 |
| T354(OY) ^{LeuT} /S323(OY) ^{MhsT} | 2.4 | 2.4 | 2.3 | 2.5 | 2.4 |
| S355(OY) ^{LeuT} /S324(OY) ^{MhsT} | 2.3 | 2.4 | 2.4 | 2.5 | 2.4 |
| HOH ^{MhsT} | – | – | – | 2.7 | 3.1 |

Supplementary References

61. Zhao, Y. et al. Substrate-dependent proton antiport in neurotransmitter:sodium symporters. *Nat Chem Biol* **6**, 109-16 (2010).
62. Forrest, L.R. & Rudnick, G. The rocking bundle: a mechanism for ion-coupled solute flux by symmetrical transporters. *Physiology (Bethesda)* **24**, 377-86 (2009).
63. Wohlers, I., Andonov, R. & Klau, G.W. DALIX: optimal DALI protein structure alignment. *IEEE/ACM Trans Comput Biol Bioinform* **10**, 26-36 (2013).
64. Hasegawa, H. & Holm, L. Advances and pitfalls of protein structural alignment. *Curr Opin Struct Biol* **19**, 341-8 (2009).